How Can We Help a Patient with a Small Failing Bioprosthesis? An In Vitro Case Study

Prem A. Midha, MS[a], Vrishank Raghav, PhD[a], Jose F. Condado, MD, MS[b], Sivakkumar Arjunon, PhD[a], Domingo E. Uceda, BS[a], Stamatios Lerakis, MD[b], Vinod H. Thourani, MD[b], Vasilis Babaliaros, MD[b], Ajit P. Yoganathan, PhD[a,*]

[a]*Georgia Institute of Technology, Atlanta, GA*
[b]*Emory University Hospitals, Atlanta, GA*

Abstract

Objectives To investigate the hemodynamic performance of a transcatheter heart valve (THV) deployed at different valve-in-valve (VIV) positions in an in-vitro model using a small surgical bioprosthesis.
Background High surgical risk patients with a failing 19 mm surgical aortic bioprosthesis are not candidates for a VIV transcatheter aortic valve replacement (TAVR) due to risk of high transvalvular pressure gradients (TVPG) and patient-prosthesis mismatch (PPM).
Methods A 19 mm stented aortic bioprosthesis was mounted into the aortic chamber of a pulseduplicator and a 23 mm low profile balloon-expandable THV was deployed (valve-in-valve) in 4 positions: normal (bottom of the THV stent aligned with the bottom of the surgical bioprosthesis sewing ring); and 3 mm, 6 mm, and 8 mm above the normal position. Under controlled hemodynamics, the effect of these THV positions on valve performance (mean TVPG, geometric orifice area (GOA), and effective orifice are (EOA)), thrombotic potential (sinus shear stress), and migration risk (pullout force and embolization flow rate) were assessed.
Results Compared to normal implantation, a progressive reduction of mean TVPG was observed with each supra-annular THV position (normal: 33.10 mmHg, 3 mm: 24.69 mmHg, 6 mm: 19.16 mmHg, and 8 mm: 12.98 mmHg; $p \leq 0.001$). Simultaneously, we observed an increase in GOA (normal: 0.83 cm^2 vs. 8 mm: 1.60 cm^2; $p \leq 0.001$) and EOA (normal: 0.80 cm^2 vs. 8 mm: 1.28 cm^2; $p \leq 0.001$), and reduction in sinus shear stresses (normal: 153 dyne/cm^2 vs. 8 mm: 40 dyne/cm^2; $p \leq 0.001$), pullout forces (normal: 1.55 N vs. 8 mm: 0.68 N; $p < 0.05$), and embolization flow rates (normal: 32.91 L/min vs. 8 mm: 26.06 L/min; $p < 0.01$).
Conclusions Supra-annular implantation of a THV in a small surgical bioprosthesis reduces mean TVPG, but may increase risk of leaflet thrombosis and valve migration. A 3-6 mm supraannular deployment could be an optimal position in these cases.

Keywords: Valve-in-valve, small bioprosthesis, transcatheter aortic valve

1. Introduction

Valve-in-valve transcather aortic valve replacement (VIV-TAVR) is a feasible treatment for patients with failing aortic bioprostheses (1). While VIV implantation may restore valve function and improve symptoms, adverse events such as elevated post-procedural gradients (28.4%), coronary obstruction (3.5%), device malpositioning (15.0%) and valve leaflet thrombosis (4%) have been reported (2, 3, 4, 5). Current transcatheter heart valves (THV) were not designed for deployment into semi-rigid bioprostheses. Patients with small surgical bioprostheses (i.e. 19 mm or 21 mm valves) are generally excluded from VIV-TAVR because of the risk of patient prosthesis mismatch (PPM). In these patients, some have experimented with alternate techniques, such as supra-annular deployment, in an attempt to bypass the geometric constraints imposed by the bioprosthesis frame and improve post-procedural gradients (6, 7, 8). However, supra-annular deployment could increase the risk of coronary obstruction (9), leaflet thrombosis from flow stagnation within the sinus region (10, 11, 12, 13, 14), and THV migration (15). This in vitro study attempts to bridge a gap in VIV-TAVR knowledge, by providing hemodynamic and potential safety parameters using a low profile balloon-expandable THV at different levels ofimplantation.

2. Methods

2.1. Flow Loop

The study was conducted in the Georgia Tech Left Heart Simulator (Figure 1), a validated pulsatile flow loop that simulates physiological and pathophysiological conditions of the heart (16, 17). The surgical bioprosthesis was mounted in the aortic chamber, which is an idealized rigid acrylic chamber designed to simulate the aortic sinus and ascending aorta (Figure 2). The chamber dimensions were based off of published average anatomical measurements (18, 19). The flow rate through the valve is adjusted through a LabVIEW (v.12.0, 2012, National Instruments Corporation; Austin, TX) triggered solenoid system that controls a bladder pump and is measured

*Wallace H Coulter Department of Biomedical Engineering
Georgia Institute of Technology and Emory University
Technology Enterprise Park, Suite 200
387 Technology Circle, Atlanta, GA 30313
Email address: ajit.yoganathan@bme.gatech.edu (Ajit P. Yoganathan, PhD)

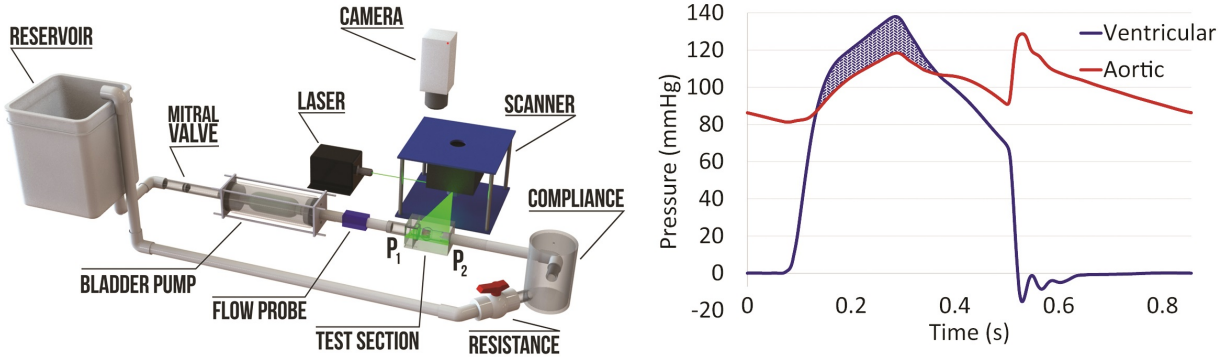

Figure 1: *In Vitro* Pulsatile Flow System - Georgia Tech Left Heart Simulator (left) used in this study is a validated pulsatile flow loop for producing physiologic and pathophysiologic conditions of the heart (16,17). Mean TVPGs were determined by the difference between ventricular and aortic pressures as shown in the shaded region (right).

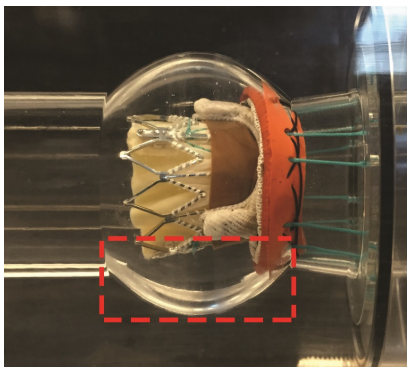

Figure 2: Aortic Chamber - The aortic chamber was designed based on published anatomical average values (18, 19). The position shown is the 8 mm VIV deployment. The dashed line indicates the region of interest for the thrombosis studies.

via an electromagnetic flow probe (600 series, Carolina Medical Electronics; East Bend, NC). Aortic and ventricular pressure waveforms (Figure 1) are tuned through a lumped systemic resistance and compliance and are measured with pressure transducers (Deltran® DPT-200, Utah Medical Products, Inc.; Midvale, UT) on either side of the valve annulus.

2.2. *Valve models and deployment*

A 23 mm balloon-expandable SAPIEN XT (Edwards Lifesciences, Irvine, CA, USA) was deployed within a 19 mm PERIMOUNT (17 mm ID, Edwards Lifesciences) in 4 positions: normal (bottom of the THV stent aligned with the bottom of the surgical bioprosthesis sewing ring); and 3 mm, 6 mm, and 8 mm above the normal position. Please note that the SAPIEN XT is considered a low profile TAVR device. In all supra-annular positions, a second balloon inflation was performed to flare the aortic end of THV ("flower pot" geometry, Figure 3).

2.3. *Hemodynamics*

Mean transvalvular pressure gradients (TVPG) were measured and used as surrogates of VIV performance. The working fluid was a 3.5 cSt saline-glycerine solution (approximately

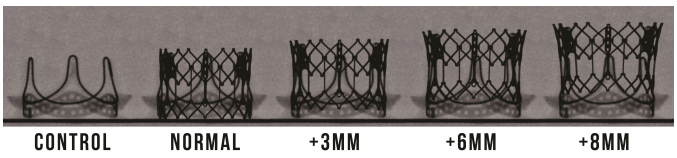

Figure 3: Deployment Schematic - Schematic representation of deployment heights as they would be seen by x-ray.

36% glycerine by volume in 0.9% NaCl) to match the kinematic viscosity of blood. The flow rate was tuned for a mean cardiac output of 5 L/min and a systolic duration of 35%. The resistance and compliance were then adjusted to ensure a diastolic aortic pressure of 80 mmHg and a systolic pressure of 120 mmHg (Figure 1). Two hundred consecutive cardiac cycles (n=200) of hemodynamic data (aortic pressure, ventricular pressure, and flow rate) were collected for each test condition at 1 kHz data sampling rate using a custom LabVIEW Virtual Instrument.

2.4. *Aortic valve orifice area*

Aortic Valve Orifice Area: GOA was determined through en face high-speed imaging via a Karl Storz 88630 SF borescope (Karl Storz, Tuttlingen, Germany) connected to a Basler A504k high-speed CCD camera (Basler Corp, Exton, PA). Four cardiac cycles (n=4) of data were collected for each implantation position. The images were manually segmented and scaled to determine peak systolic GOA (Figure 4). Effective orifice area (EOA) was computed through the Gorlin equation (20).

$$EOA = \frac{Q}{51.6\sqrt{TVPG}} \tag{1}$$

2.5. *Thrombosis risk*

High-speed particle image velocimetry (PIV) experiments were conducted using the flow system described above. The purpose of these PIV experiments was to obtain time-resolved measurements of the flow velocities in the sinus (Figure 2) as a means of assessing relative risk of stagnation-induced thrombosis. A diode-pumped solid-state laser (Shenzhen Optolaser,

Figure 4: En Face View Example - High-speed en face imaging of the VIV allows for analytical computation of the fluid forces acting upon the THV.

2W, 532 nm) was utilized as the light source, a custom LaVision scanner was used to convert the continuous beam into a high frequency pulse, and a CMOS camera (Vision Research Phantom Miro M/R/LC123, 1920×1200 pixels, 730 fps) was used to image the particles in a single plane. Fluorescent polymeric rhodamine-B particles of diameters 1-20 μm were used as seeding particles to visualize the flow field under laser illumination. The resultant velocity field in the sinus was used to calculate the viscous shear stress (VSS) field throughout the cardiac cycle and is given by the following expression:

$$VSS = \mu\left(\frac{\partial u}{\partial y} + \frac{\partial v}{\partial x}\right) \quad (2)$$

The VSS data presented in this work is computed over 9 cardiac cycles (n=9). This velocity field dependent measure is critically linked to thrombotic potential of the leaflets of the valve (21, 22).

2.6. Pullout forces

The pullout force was measured as a means of determining the relative embolization risk for each VIV implantation position. The bioprosthesis was sutured to the bottom of a rigid acrylic chamber filled with saline using 2.0 Ethibond sutures (Ethicon US, Somerville, NJ, USA). A single continuous 2.0 Ethibond suture was also attached to the THV stent at 3 equally spaced locations to ensure equally distributed tension (Figure 5). The THV was then deployed into the surgical bioprosthesis at the desired location. The THV harness was attached to a Mark-10 Series 3 digital force gauge which records at 10 Hz. Force was applied gradually until the valve migrated and the force measured by the gauge decreased. Due to the flower pot configuration of the THV, the primary concern was antegrade migration into the ascending aorta. Each test condition was repeated 4 times (n=4).

2.7. Embolization flow rate

In addition to pullout forces, embolization risk was assessed by subjecting each THV deployment to gradually increasing steady antegrade flow. The flow rate at which each THV deployment embolized was recorded. Each test was repeated 4 times (n=4).

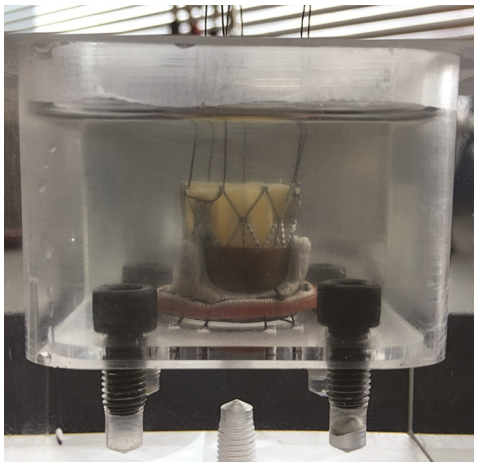

Figure 5: Pullout Force Chamber - The pullout force chamber is a rigid housing filled with saline in which the surgical bioprosthesis is securely sutured. The THV is deployed at the desired location and then pulled by a uniaxial digital force gauge.

2.8. Statistical analysis

The data is presented as a mean standard deviation. Normality of all the data was tested using the Anderson-Darling method. One-way ANOVA was used for analyzing independent sample sets with Tukeys post-hoc test for comparisons between multiple groups. The pullout force data were not normally distributed, and therefore, a Mann-Whitney U test was used instead. P-values less than 0.05 were considered statistically significant and the analysis was done using SPSS Statistics for Mac (Version 20.0, IBM Corp, NY).

3. Results

3.1. Hemodynamics

The TVPG is reported as a mean measured over two hundred cycles of gathered data (Figure 6). The dashed red line indicates the threshold for device success as defined by VARC-2 and AHA/ACC guidelines (23, 24). As expected, our normal VIV position resulted in a significantly higher mean TVPG than the surgical bioprosthesis alone (33.10 ± 0.37 mmHg vs. 13.07 ± 0.16 mmHg; p<0.001). These TVPG progressively decreased with each supra-annular implantation to 24.69 ± 0.38 mmHg, 19.16 ± 0.26 mmHg and 12.98 ± 0.25 mmHg at supra-annular 3 mm, 6 mm and 8 mm, respectively. At 8 mm above normal implantation, the mean TVPG was similar to the control case, and was the lowest TVPG for any VIV position. The reduction in mean TVPG with increasingly supra-annular VIV deployment was primarily due to increases in GOA (Figure 7) through further flaring of the THV (more exaggerated flower pot geometry). The dashed line on the figure indicates the threshold for severe aortic valve stenosis (24). The GOA of the control case was 1.78 ± 0.01 cm^2 and dropped to 0.83 ± 0.01 cm^2 after deployment in the normal position (p<0.001). At successively supra-annular positions, the GOA increased from 0.99 ± 0.01 cm^2 to 1.2 ± 0.01 cm^2 1.6 ± 0.02 cm^2 (p<0.001).

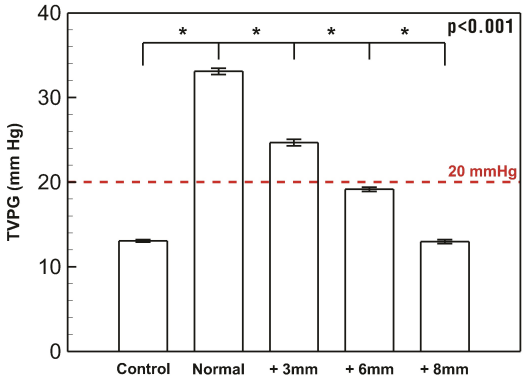

Figure 6: Mean Transvalvular Pressure Gradients - Increasingly supra-annular THV deployment yields increasingly more favorable mean TVPGs. The dashed red line indicates the threshold for mild aortic stenosis. The error bars indicate standard deviation and all p-values are less than 0.001.

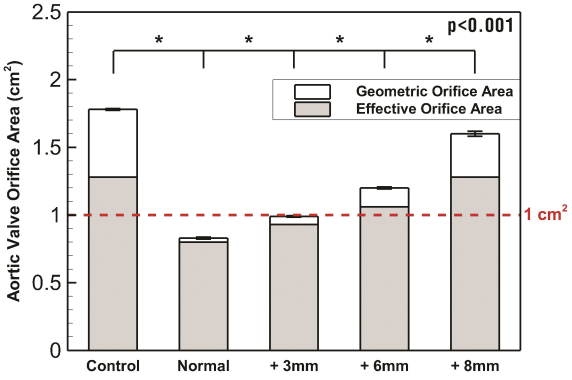

Figure 7: Aortic Valve Area - Supra-annular THV deployment resulted in increased GOA and EOA. The dashed line indicates the threshold for severe aortic valve stenosis (24). The error bars indicate standard deviation and all p-values are less than 0.001.

3.2. *Thrombosis risk*

The VSS results are maximum values obtained after spatial integration of the shear stress fields over the area of the sinus at each time point in the cardiac cycle. Figure 8 illustrates the variation of maximum VSS among THV deployments. It was observed that the VSS decreases with increasing deployment height of the THV ranging from 1.53 ± 0.21 dyne/cm^2 to 0.40 ± 0.10 dyne/cm^2 (p<0.01). Given that human blood has been shown to form aggregates at shear rates under 46 s^{-1} (1.61 dyne/cm^2), the stagnation-induced thrombosis safety threshold lies above all VIV deployments (14).

3.3. *Pullout forces*

The pullout forces are reported as a mean and standard deviation. With each successive supra-annular deployment, the contact area between the THV and SAVR reduced, resulting in lower required force for migration. While the THV did not migrate under physiologic pulsatile flow conditions at any of

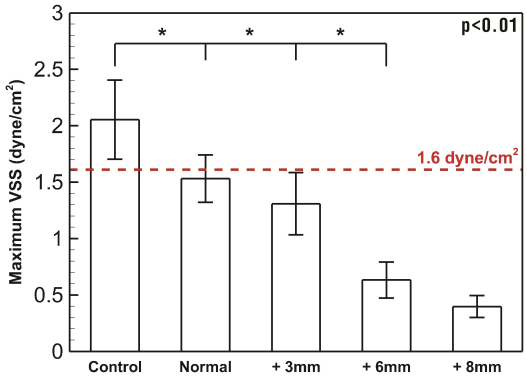

Figure 8: Sinus Flow (Viscous Shear Stress) - The maximum VSS over the cardiac cycle decreases with increasingly supra-annular THV deployment. The error bars indicate standard deviation and all p-values are less than 0.01.

the deployment positions, the measured pullout force reduced drastically between normal and 3 mm supra-annular deployment positions (1.55 N vs. 0.9125 N; p=0.029), and steadily reduced across the 3 mm to 8 mm positions as shown in Figure 9 (p<0.06). In this study, migration into the left ventricle was not a concern because the supra-annular implantation provides additional geometric resistance under retrograde flow. Dwyer et al. derived estimates of fluid forces on a transcatheter valve based on pressure gradients, viscous forces, and momentum changes, and showed that pressure forces accounted for approximately 75% of the total forces (25). Based on these results, a baseline safety threshold was computed (Figure 9).

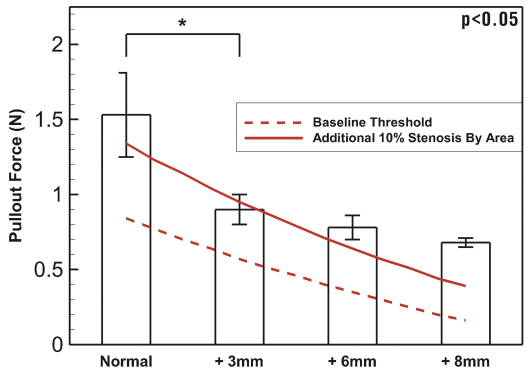

Figure 9: Pullout Forces - The magnitude of force required to dislodge the THV in VIV is plotted as the pullout force measured by a digital force gauge. The dashed red line indicates the analytically derived fluid forces experienced by a THV in VIV. The solid red line indicates the fluid forces on the same deployment if it were to undergo 10% more stenosis by area. The error bars indicate standard deviation and all p-values are less than 0.05.

$$\text{Total Fluid force} = \frac{TVPG \times A}{0.75} \qquad A = GOA_{SAVR} - GOA_{TAVR} \tag{3}$$

Table 1: Compiled results - results are represented as mean and standard deviations compared against a threshold value. Results in red did not meet the threshold criterion

	Sample size (n)	Safety threshold	Control	Normal	+3mm	+6mm	+8mm
Mean TVPG (mmHg), Mean (SD)	200	20	13.07 (0.16)	33.10 (0.37)	24.69 (0.38)	19.16 (0.26)	12.98 (0.25)
GOA (cm^2), Mean (SD)	4	1	1.78 (0.01)	0.83 (0.01)	0.99 (0.01)	1.20 (0.01)	1.60 (0.02)
EOA (cm^2), Mean (SD)	200	1	1.28 (0.01)	0.80 (<0.01)	0.93 (<0.01)	1.06 (<0.01)	1.28 (0.01)
Max VSS (dyn/cm^2), Mean (SD)	9	1.61	2.05 (0.35)	1.53 (0.21)	1.31 (0.28)	0.63 (0.16)	0.40 (0.10)
Pullout force (N), Mean (SD)	4	Figure 9	-	1.55 (0.20)	0.91 (0.07)	0.76 (0.06)	0.68 (0.02)
Embolization flow rate (L/min), Mean (SD)	4	30	-	32.91 (0.85)	31.57 (0.75)	29.37 (0.73)	26.06 (1.27)

where GOA_{SAVR} is the maximum surgical bioprosthesis GOA based on the internal diameter of the valve, and GOA_{TAVR} is the geometric orifice area determined via en face imaging of the deployed THV (Figure 4). This threshold represents the theoretical lower limit of pullout force necessary to avoid embolization. Applying a theoretical additional 10% stenosis by area to this threshold yields the upper safety threshold shown in Figure 9. It should be noted that the 3 mm implantation position does not meet this upper safety threshold.

3.4. Embolization flow rate

The embolization flow rates follow a similar trend as the pullout forces, though the separation between deployments is not as distinct (Figure 10). The normal deployment embolized at 32.91 ± 0.85 L/min, while the supra-annular deployments of 3 mm, 6 mm, and 8 mm embolized at 31.57 ± 0.75 L/min, 29.37 ± 0.73 L/min, and 26.06 ± 1.27 L/min, respectively. The safety threshold of 30 L/min was defined by a peak instantaneous systolic flow rate through the aortic valve in a healthy adult with a cardiac output of 5 to 6 L/min (26). Most TAVR patients have some degree of impaired cardiac output, making 30 L/min peak instantaneous flow rate a fairly conservative threshold.

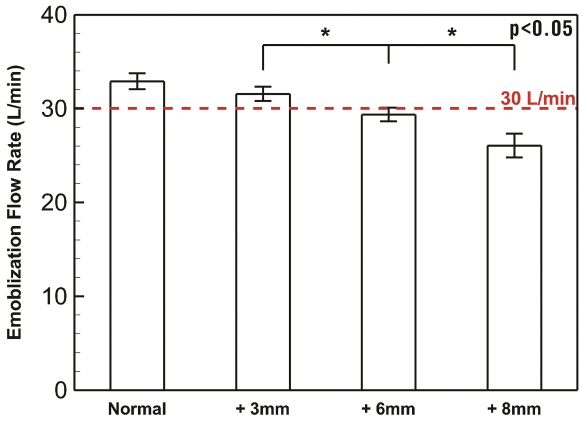

Figure 10: Embolization Flow Rates - Each VIV deployment was subjected to gradually increasing steady flow until the THV embolized. The error bars indicate standard deviation and all indicated p-values are less than 0.05.

4. Discussion

The results of this study (Table 1) suggest that supra-annular THV implantation can lead to lower mean TVPG than a normal implantation after a VIV-TAVR in patients with a small surgical bioprosthesis (~19 mm). We found that increasingly supra-annular deployment resulted in even lower TVPG, ultimately reaching the similar values to our control (normal functioning bioprosthetic valve). This improvement of gradients can be explained by a better expansion of the downstream portion of the THV at supra-annular locations, demonstrated by the larger GOA measurements and EOA calculations at these levels. Thus, a high implantation VIV-TAVR could be performed with good outcomes in high surgical risk patients that, to this date, are not considered candidates because of the size of their original surgical bioprosthesis. Moreover, prior clinical registries have reported that VIV-TAVR in patients with small surgical bioprostheses (defined as ≤21 mm) have higher mortality than patients with larger surgical bioprostheses that undergo this same procedure, mostly because the former are associated with an increased rate of PPM and elevated TVPG (27). While this study focused only on the hemodynamics of a high-implantation VIV-TAVR in a 19 mm surgical bioprosthesis, we propose that such a procedure may benefit patients with other surgical bioprosthesis sizes.

The observed benefit of high THV implantation measured by mean TVPG could be eclipsed by an increased risk of leaflet thrombosis. Increasingly supra-annular deployment resulted in reduced sinus velocities and VSS levels, which could increase the risk of leaflet thrombosis from flow stagnation (13, 14). Recent evidence suggest that thrombosis is an underreported prob-

lem affecting THVs. However, the pathophysiology of this process is poorly understood, with most thrombus deposition occurring on the valve leaflets (5, 28, 29, 30). Though none of our VIV-TAVR deployments positions yielded VSS levels above the currently understood safety threshold values for thrombus formation, the exact clinical significance of this flow stagnation remains unclear and needs further investigation. Traditionally, thrombosis is discussed in terms of Virchow's triad (materials, biochemistry, and fluid flow), and the conditions that impact thrombosis risk are highly patient-specific. Our in vitro model did not incorporate factors such as aortic distensibility or coronary flow and does not account for patient specific anatomy or physiology that can alter thrombosis risk. As the intention of our study was to understand the fluid mechanics and hemodynamic implications of an alternate deployment, we focused on inspecting the differences observed in thrombosis risk based strictly on fluid mechanics metrics.

We also observed that supra-annular THV implantation resulted in a reduction of force necessary to dislodge the THV. Interestingly, we found that the largest drop in pull-out force occurred between the normal and the 3 mm deployments, possibly because of a reduction of the contact area with the internal surface of the surgical bioprosthesis suture cuff. The coefficient of friction between the THV stent and the surgical bioprosthesis suture cuff is likely substantially higher than between the THV stent and the surgical bioprosthesis leaflets. Therefore, there is a gradual decrease in the pullout force at further supra-annular positions where the contact area of the THV stent with the suture cuff is minimal. Though these lower forces could translate to an increased risk for valve migration, especially in situations of high cardiac output, the calculated (and conservative) baseline safety threshold for valve migration was never reached under physiologic pulsatile flow conditions even at the highest THV implantation (8 mm). Furthermore, the commonly seen calcification and fibrosis in failing bioprostheses is likely to increase the amount of force required to dislodge the THV in a patient. Suggesting that in a worst-case scenario, though possible, antegrade THV embolization is unlikely to occur.

Based on this in vitro evidence and threshold values, the authors would recommend a deployment of a SAPIEN XT valve between 3 mm and 6 mm supra-annular in a patient with a failing 19 mm PERIMOUNT. While the authors acknowledge the limitations of this study, they would like to emphasize that clinicians must consider patient-specific anatomic characteristics and carefully weigh the benefit of high THV implantation in reducing post-procedural gradients, against the potential risk for valve leaflet thrombosis and device migration in potential candidates for VIV-TAVR. Similar in vitro studies utilizing other surgical bioprostheses and TAVR devices, including the Medtronic CoreValve, are critically important to optimize VIV performance and patient outcomes.

5. Acknowledgments

The authors would like to acknowledge the members of the Cardiovascular Fluid Mechanics Laboratory for their assistance and feedback. The work at the Cardiovascular Fluid Mechanics Laboratory at the Georgia Institute of Technology was funded through discretionary funds available to the Principal Investigator through the Wallace H Coulter Endowed Chair.

References

[1] Kishore J Harjai, Jean-Michel Paradis, and Susheel Kodali. Transcatheter aortic valve replacement: Game-changing innovation for patients with aortic stenosis. *Annual review of medicine*, 65:367–383, 2014.

[2] Ali N Azadani, Nicolas Jaussaud, Peter B Matthews, Liang Ge, Timothy AM Chuter, and Elaine E Tseng. Transcatheter aortic valves inadequately relieve stenosis in small degenerated bioprostheses. *Interactive cardiovascular and thoracic surgery*, 11(1):70–77, 2010.

[3] Danny Dvir, Marco Barbanti, John Tan, and John G Webb. Transcatheter aortic valve-in-valve implantation for patients with degenerative surgical bioprosthetic valves. *Current problems in cardiology*, 39(1):7–27, 2014.

[4] Tina Leetmaa, Nicolaj C Hansson, Jonathon Leipsic, Kaare Jensen, Steen H Poulsen, Henning R Andersen, Jesper M Jensen, John Webb, Philipp Blanke, Mariann Tang, et al. Early aortic transcatheter heart valve thrombosis diagnostic value of contrast-enhanced multidetector computed tomography. *Circulation: Cardiovascular Interventions*, 8(4):e001596, 2015.

[5] Eduardo De Marchena, Julian Mesa, Sydney Pomenti, Christian Marin y Kall, Ximena Marincic, Kazuyuki Yahagi, Elena Ladich, Robert Kutz, Yaar Aga, Michael Ragosta, et al. Thrombus formation following transcatheter aortic valve replacement. *JACC: Cardiovascular Interventions*, 8(5):728–739, 2015.

[6] Ali N Azadani, Nicolas Jaussaud, Peter B Matthews, Liang Ge, T Sloane Guy, Timothy AM Chuter, and Elaine E Tseng. Valve-in-valve implantation using a novel supravalvular transcatheter aortic valve: proof of concept. *The Annals of thoracic surgery*, 88(6):1864–1869, 2009.

[7] D Tanase, J Grohmann, S Schubert, F Uhlemann, A Eicken, and P Ewert. Cracking the ring of edwards perimount bioprosthesis with ultrahigh pressure balloons prior to transcatheter valve in valve implantation. *International journal of cardiology*, 176(3):1048–1049, 2014.

[8] Florent Chevalier, Jonathon Leipsic, and Philippe Généreux. Valve-in-valve implantation with a 23-mm balloon-expandable transcatheter heart valve for the treatment of a 19-mm stentless bioprosthesis severe aortic regurgitation using a strategy of extreme underfilling. *Catheterization and Cardiovascular Interventions*, 84(3):503–508, 2014.

[9] Danny Dvir, Jonathon Leipsic, Philipp Blanke, Henrique B Ribeiro, Ran Kornowski, Augusto Pichard, Joseph Rodés-Cabau, David A Wood, Dion Stub, Itsik Ben-Dor, et al. Coronary obstruction in transcatheter aortic valve-in-valve implantation preprocedural evaluation, device selection, protection, and treatment. *Circulation: Cardiovascular Interventions*, 8(1):e002079, 2015.

[10] Ahmad Falahatpisheh and Arash Kheradvar. High-speed particle image velocimetry to assess cardiac fluid dynamics in vitro: From performance to validation. *European Journal of Mechanics-B/Fluids*, 35:2–8, 2012.

[11] Maud B Gorbet and Michael V Sefton. Biomaterial-associated thrombosis: roles of coagulation factors, complement, platelets and leukocytes. *Biomaterials*, 25(26):5681–5703, 2004.

[12] JEFFREY A Hubbell and LARRY V McIntire. Platelet active concentration profiles near growing thrombi. a mathematical consideration. *Biophysical journal*, 50(5):937, 1986.

[13] David N Ku. Blood flow in arteries. *Annual Review of Fluid Mechanics*, 29(1):399–434, 1997.

[14] H Schmid-Schönbein, P Gaehtgens, and H Hirsch. On the shear rate dependence of red cell aggregation in vitro. *Journal of Clinical Investigation*, 47(6):1447, 1968.

[15] Vinayak Vinnie Nilkanth Bapat, Feras Khaliel, and Leo Ihleberg. Delayed migration of sapien valve following a transcatheter mitral valve-in-valve implantation. *Catheterization and Cardiovascular Interventions*, 83(1):E150–E154, 2014.

[16] Jean-Pierre Rabbah, Neelakantan Saikrishnan, and Ajit P Yoganathan. A novel left heart simulator for the multi-modality characterization of native mitral valve geometry and fluid mechanics. *Annals of biomedical engineering*, 41(2):305–315, 2013.

[17] Andrew W Siefert, Jean Pierre M Rabbah, Kevin J Koomalsingh, Steven A Touchton, Neelakantan Saikrishnan, Jeremy R McGarvey,

Robert C Gorman, Joseph H Gorman, and Ajit P Yoganathan. In vitro mitral valve simulator mimics systolic valvular function of chronic ischemic mitral regurgitation ovine model. *The Annals of thoracic surgery*, 95(3):825–830, 2013.

[18] Joseph Knight, Vartan Kurtcuoglu, Karl Muffly, William Marshall Jr, Paul Stolzmann, Lotus Desbiolles, Burkhardt Seifert, Dimos Poulikakos, and Hatem Alkadhi. Ex vivo and in vivo coronary ostial locations in humans. *Surgical and radiologic anatomy*, 31(8):597–604, 2009.

[19] H Reul, A Vahlbruch, M Giersiepen, TH Schmitz-Rode, V Hirtz, and S Effert. The geometry of the aortic root in health, at valve disease and after valve replacement. *Journal of biomechanics*, 23(2):181–191, 1990.

[20] Neelakantan Saikrishnan, Gautam Kumar, Fadi J Sawaya, Stamatios Lerakis, and Ajit P Yoganathan. Accurate assessment of aortic stenosis a review of diagnostic modalities and hemodynamics. *Circulation*, 129(2):244–253, 2014.

[21] Elliott M Groves, Ahmad Falahatpisheh, Jimmy L Su, and Arash Kheradvar. The effects of positioning of transcatheter aortic valves on fluid dynamics of the aortic root. *ASAIO Journal*, 60(5):545–552, 2014.

[22] Neelakantan Saikrishnan, Choon-Hwai Yap, Nicole C Milligan, Nikolay V Vasilyev, and Ajit P Yoganathan. In vitro characterization of bicuspid aortic valve hemodynamics using particle image velocimetry. *Annals of biomedical engineering*, 40(8):1760–1775, 2012.

[23] A Pieter Kappetein, Stuart J Head, Philippe Généreux, Nicolo Piazza, Nicolas M van Mieghem, Eugene H Blackstone, Thomas G Brott, David J Cohen, Donald E Cutlip, Gerrit-Anne van Es, et al. Updated standardized endpoint definitions for transcatheter aortic valve implantation: The valve academic research consortium-2 consensus document. *Journal of the American College of Cardiology*, 60(15):1438–1454, 2012.

[24] Rick A Nishimura, Catherine M Otto, Robert O Bonow, Blase A Carabello, John P Erwin, Robert A Guyton, Patrick T OGara, Carlos E Ruiz, Nikolaos J Skubas, Paul Sorajja, et al. 2014 aha/acc guideline for the management of patients with valvular heart disease: a report of the american college of cardiology/american heart association task force on practice guidelines. *Journal of the American College of Cardiology*, 63(22):e57–e185, 2014.

[25] Harry A Dwyer, Peter B Matthews, Ali Azadani, Liang Ge, T Sloane Guy, and Elaine E Tseng. Migration forces of transcatheter aortic valves in patients with noncalcific aortic insufficiency. *The Journal of thoracic and cardiovascular surgery*, 138(5):1227–1233, 2009.

[26] Walter F Boron and Emile L Boulpaep. *Medical Physiology, 2e Updated Edition: with STUDENT CONSULT Online Access*. Elsevier Health Sciences, 2012.

[27] Danny Dvir, John G Webb, Sabine Bleiziffer, Miralem Pasic, Ron Waksman, Susheel Kodali, Marco Barbanti, Azeem Latib, Ulrich Schaefer, Josep Rodés-Cabau, et al. Transcatheter aortic valve implantation in failed bioprosthetic surgical valves. *JAMA*, 312(2):162–170, 2014.

[28] Lawrence N Scotten and Rolland Siegel. Importance of shear in prosthetic valve closure dynamics. *The Journal of heart valve disease*, 20(6):664–672, 2011.

[29] Doreen Richardt, Thorsten Hanke, and Hans-Hinrich Sievers. Two cases of heart failure after implantation of a corevalve prosthesis. *The New England journal of medicine*, 372(11):1079–1080, 2015.

[30] Gloria Faerber, Simone Schleger, Mahmoud Diab, Martin Breuer, Hans R Figulla, Walter B Eichinger, and Torsten Doenst. Valve-in-valve transcatheter aortic valve implantation: The new playground for prosthesis-patient mismatch. *Journal of interventional cardiology*, 27(3):287–292, 2014.